Archival Report

Biological Psychiatry

Microglial Acid Sensing Regulates Carbon Dioxide-Evoked Fear

Lauren Larke Vollmer, Sriparna Ghosal, Jennifer L. McGuire, Rebecca L. Ahlbrand, Ke-Yong Li, Joseph M. Santin, Christine A. Ratliff-Rang, Luis G.A. Patrone, Jennifer Rush, Ian P. Lewkowich, James P. Herman, Robert W. Putnam, and Renu Sah

ABSTRACT

BACKGROUND: Carbon dioxide (CO_2) inhalation, a biological challenge and pathologic marker in panic disorder, evokes intense fear and panic attacks in susceptible individuals. The molecular identity and anatomic location of CO_2-sensing systems that translate CO_2-evoked fear remain unclear. We investigated contributions of microglial acid sensor T cell death–associated gene-8 (TDAG8) and microglial proinflammatory responses in CO_2-evoked behavioral and physiological responses.

METHODS: CO_2-evoked freezing, autonomic, and respiratory responses were assessed in TDAG8-deficient ($^{-/-}$) and wild-type ($^{+/+}$) mice. Involvement of TDAG8-dependent microglial activation and proinflammatory cytokine interleukin (IL)-1β with CO_2-evoked responses was investigated using microglial blocker, minocycline, and IL-1β antagonist IL-1RA. CO_2-chemosensitive firing responses using single-cell patch clamping were measured in TDAG8$^{-/-}$ and TDAG8$^{+/+}$ mice to gain functional insights.

RESULTS: TDAG8 expression was localized in microglia enriched within the sensory circumventricular organs. TDAG8$^{-/-}$ mice displayed attenuated CO_2-evoked freezing and sympathetic responses. TDAG8 deficiency was associated with reduced microglial activation and proinflammatory cytokine IL-1β within the subfornical organ. Central infusion of microglial activation blocker minocycline and IL-1β antagonist IL-1RA attenuated CO_2-evoked freezing. Finally, CO_2-evoked neuronal firing in patch-clamped subfornical organ neurons was dependent on acid sensor TDAG8 and IL-1β.

CONCLUSIONS: Our data identify TDAG8-dependent microglial acid sensing as a unique chemosensor for detecting and translating hypercapnia to fear-associated behavioral and physiological responses, providing a novel mechanism for homeostatic threat detection of relevance to psychiatric conditions such as panic disorder.

Keywords: Acid sensing, Carbon dioxide, Fear, Microglia, Panic, TDAG8

http://dx.doi.org/10.1016/j.biopsych.2016.04.022

Fear encompasses threat-associated behavioral and physiological responses crucial to survival. Most of our current biological understanding of fear genesis comes from studies in which animals are exposed to exteroceptive aversive stimuli such as pain or predator exposure (1,2). Fear responses also can be evoked by stimuli producing an internal threat to homeostasis and imminent danger to survival. A widely studied interoceptive stimulus, carbon dioxide (CO_2) inhalation, produces intense fear, autonomic, and respiratory responses that can evoke panic attacks. In humans, CO_2 sensitivity lies on a continuum (3), with panic disorder (PD) patients being highly sensitive to low CO_2 doses, whereas healthy volunteers experience panic-like symptoms only at higher concentrations (4,5). In the extracellular space, CO_2 combines with water to produce protons, leading to systemic acidosis (6,7), which is responsible for the panicogenic effects of CO_2. Prior studies indicate that acid-sensing ion channels in the amygdala contribute to CO_2-evoked fear responses (8). However, recent studies in patients with amygdala damage resulting from Urbach-Wiethe disease indicate that the amygdala is not required for the expression of fear and panic to CO_2 inhalation (9), suggesting that distinct chemosensory systems may exist for homeostatic threats such as CO_2 that may not engage traditional fear mechanisms.

Microglia, innate immune cells of the central nervous system (CNS) (10), are recruited in physiological responses to homeostatic fluctuations (11). Microglia transform rapidly from a resting to a proinflammatory activated state on sensing subtle imbalance in ionic homeostasis (12,13), in accordance with their role in maintenance of the CNS microenvironment. Extracellular acidification induces rapid alteration in microglial morphologic features and actin integrity (14,15), suggesting their potential engagement in the effects of acidotic stimuli such as CO_2. This study addresses possible mechanisms responsible for generation of panic-relevant fear responses, focusing on the T cell death–associated gene-8 (TDAG8), an acid-sensing G-protein coupled receptor (16,17). TDAG8 is expressed in microglial cells resident in sensory

SEE COMMENTARY ON PAGE e47

ISSN: 0006-3223

circumventricular organs (CVOs). Sensory CVOs such as the subfornical organ (SFO) are integrative sites lacking a blood-brain barrier and have access to systemic and CNS compartments for maintenance of homeostasis (18). Importantly, the SFO has been identified as a site where interoceptive stimuli can be sensed and relayed to panic-generating CNS areas (19). Previous work associates the SFO with panic-like responses to intravenous lactate (20,21). The SFO therefore may be a primary locus for detecting interoceptive challenges relevant to panic. Given the expression of microglial acid-sensor TDAG8 in a panic-regulatory area, we investigated potential recruitment of the receptor in CO_2-evoked behavior and physiological features. We hypothesized that acid-sensor TDAG8-mediated microglial activation within the SFO contributes to the behavioral and physiological sequelae of CO_2 inhalation. Our data suggest that acid-sensor TDAG8 acts in the SFO to promote CO_2-evoked behavioral (freezing) and physiological (cardiovascular) responses via a mechanism involving microglial activation and the proinflammatory cytokine interleukin (IL)-1β.

METHODS AND MATERIALS

Animals

$TDAG8^{-/-}$ mice, a generous gift from Dr. Owen Witte, University of California at Los Angeles, were generated on a BALB/c background (22). All experiments reported here were performed on 8- to- 16-week-old homozygous male mice carrying wild-type ($TDAG8^{+/+}$) or knockout ($TDAG8^{-/-}$) allele. All behavioral experiments were performed between 8 AM and 1 PM during the 12-hour light cycle. Study protocols were approved by the Institutional Animal Care and Use Committees of University of Cincinnati and Wright State University, in vivariums accredited by the Association for Assessment and Accreditation of Laboratory Animal Care.

Carbon Dioxide Behavior Studies

Experimental layout is shown in Figure 2A (details in the Supplement). Mice were habituated to the CO_2 chamber for 10 minutes 1 day before the CO_2 challenge (day 0). On day 1, mice were exposed to air and 5% and 10% CO_2 concentrations for 10 minutes, during which behavior was videotaped. This CO_2 concentration range is translationally relevant to challenge studies in humans (5). The following day (day 2), animals were returned to the chamber for 5 minutes in the absence of CO_2. Freezing, defined as the complete lack of movement except for respiration, was scored using the FreezeScan software (CleverSys, Inc., Reston, VA) by a trained observer blinded to genotype and treatment. After an initial dose-response study, all subsequent experiments were conducted using 5% CO_2.

Radiotelemetry Surgery and Recording

Mice were implanted with telemetric devices (PA-C20; Data Sciences International, New Brighton, MN) to measure blood pressure (BP) and heart rate. To assess responses to CO_2 inhalation, the data were analyzed as response during CO_2 inhalation minus average response 10 minutes before CO_2 inhalation. This is consistent with clinical studies in which cardiovascular effects during CO_2 inhalation were analyzed over baseline pre-exposure measurements (23). For measurements during day 2 context exposure, delta of mean response was calculated over baseline (average of 2 hours before entry into the room) as described previously (24).

Whole-Body Plethysmography

Ventilatory parameters in unrestrained, nonanesthetized mice were measured using whole-body plethysmography, as described previously (25) with modifications. For setup and data collection details, see the Supplement.

Drug Administration

Minocycline (10 μg/500 nL; Sigma-Aldrich, St. Louis, MO) was administered intracerebroventricularly once daily for 4 days before CO_2-inhalation exposure. For the minocycline–IL-1β experiment, IL-1β (5 ng/500 nL; R&D Systems, Minneapolis, MN) was administered to minocycline-treated mice 20 minutes before CO_2 inhalation. For IL-1β necessity and sufficiency experiments, mouse recombinant IL-1RA [an endogenous receptor antagonist that binds selectively to the IL-1 receptor (IL-1R) and prevents signaling via this receptor (1.8 μg/2 μL; R&D Systems)] or IL-1β itself (5 ng/500 nL) was administered 20 minutes before CO_2 or air inhalation, respectively. Doses and duration of minocycline, IL-1RA, and IL-1β were adapted from previous studies (26–28). For surgery details, see the Supplement.

Immunofluorescence

Coronal brain sections were immunolabeled with primary antibodies against green fluorescent protein (GFP) (1:3000; cat. no. A-11122; Invitrogen, Grand Island, NY), anti-ionized calcium binding adapter molecule (1:1000; cat. no. 234-003; Synaptic Systems, Inc., Gottingen, Germany), anti-HuC/D (1:200; cat. no. A-21271; Invitrogen), anti-glial fibrillary acidic protein (1:1000; cat no. ab4674; Abcam, Cambridge, MA) using standard immunofluorescence procedures (see the Supplement for details).

Morphologic Analysis

Methodology to measure morphologic changes in microglia after CO_2 inhalation was adapted from previous studies (29,30). Flattened images from Z-stacks were examined using ImageJ software (National Institutes of Health, Bethesda, MD) to quantify increased soma perimeter and attenuated microglial branching complexity and process length (deramification) that are parameters for assessing microglial activation. (For details, see the Supplement.)

Measurement of Cytokines

Cytokine concentrations were measured using the Bio-Plex Mouse Cytokine Assays (Bio-Rad, Hercules, CA). For details on tissue collection, see the Supplement.

Slice Electrophysiology

Coronal SFO slices (300 μm) were used for whole-cell patch clamp recordings of CO_2-evoked neuronal firing as

described (31). The chemosensitive response of a neuron was determined by measuring the change in firing rate in response to a hypercapnic acidotic solution of artificial cerebrospinal fluid (aCSF) equilibrated with either 7.5% CO_2 (pH, 7.3) or 10% CO_2 (pH, 7.15). If the firing rate of a neuron increased by more than 20%, it was deemed to be chemosensitive; otherwise, it was classified as nonchemosensitive as described (31) (for methodologic details, see the Supplement).

Data Analysis and Statistics

Data are presented as mean ± SEM. Normality was tested formally for all data and met assumptions of the statistical tests being used. Animals were excluded from the analysis if they were identified as outliers using Grubb's analysis, had unstable baseline recordings (telemetry), or were surgical "misses" as identified by cresyl staining. Planned comparisons were carried out using 2-tailed unpaired *t* tests to determine statistical significance between genotypes. An analysis of variance (ANOVA) was used for analysis of genotype and treatment effects. Bonferroni's post hoc analysis was applied where main effects were significant. The multiple *t* test analysis with Sidak-Bonferroni correction for multiple comparison was used for analysis of cardiovascular data. See the Supplement for details on electrophysiological and plethysmographic data analysis. *p* values less than .05 were considered significant. Prism software was used for statistical analysis (GraphPad Software, Inc., La Jolla, CA).

RESULTS

Acid-Sensor TDAG8 Is Expressed on Microglia: Expression in Sensory CVOs and Regulation by CO_2 Inhalation

Cells expressing GFP downstream of the TDAG8 promoter were identified as microglia, verified by colocalization with ionized calcium-binding adapter protein, but not with HuC/D (neurons) or glial fibrillary acidic protein (astrocytes) producing cells (Figure 1). GFP^{+ve}–ionized calcium binding adapter $molecule^{+ve}$ microglia were expressed predominantly in sensory CVOs, including the SFO (Figure 1), organ vasculosum laminae terminalis (OVLT; Supplemental Figure S1), and area postrema (Supplemental Figure S1). GFP^{+ve} cells were not evident in areas relevant to fear regulation such as the amygdala, prefrontal cortex, and periaqueductal gray (Supplemental Figure S2). TDAG8 promoter-controlled GFP expression was increased significantly in the SFO 24 hours after CO_2 inhalation (Figure 1I–K, unpaired *t* test, $t_{15} = 2.177$; $p < .05$ vs. air), but not in the area postrema or OVLT (Supplemental Figure S1Q–R; $p > .05$ vs. air), suggesting

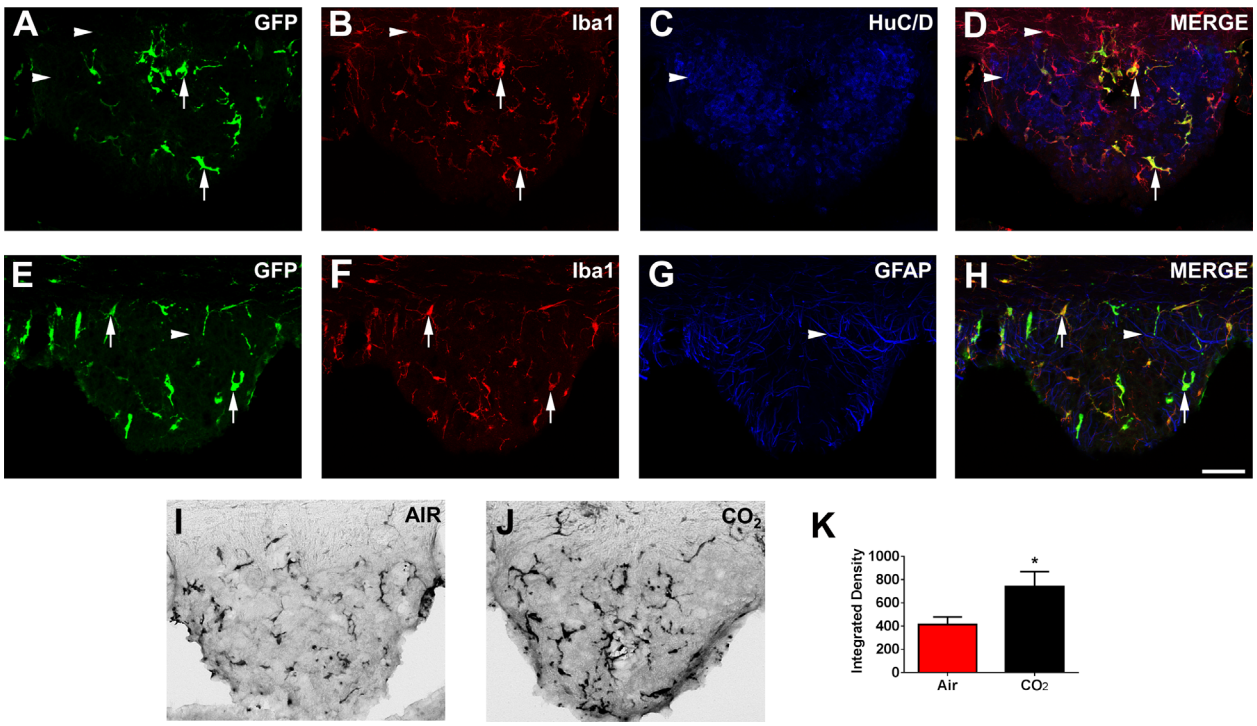

Figure 1. **(A–H)** Microglia within the sensory circumventricular organ, subfornical organ (SFO), express acid-sensing T cell death–associated gene-8 (TDAG8) receptor. **(I–K)** Regulation after carbon dioxide (CO_2) inhalation. **(A)** Using green fluorescent protein (GFP) knocked-in downstream of the TDAG8 promoter, abundant expression was localized in the SFO. **(B, D, F, H)** Cellular phenotyping using triple immunohistochemistry revealed colocalization of GFP with ionized calcium-binding adapter molecule (IBA1)-positive cells within the SFO, but not with **(C, D)** neuron-specific marker, HuC/D, or **(G, H)** astrocytic marker, glial fibrillary acidic protein (GFAP). **(I–K)** Inhalation of 5% CO_2 evoked a significant upregulation of TDAG8 promoter-regulated GFP expression within the SFO area. Representative images showing GFP-positive cells after **(I)** air inhalation and **(J)** CO_2 inhalation. **(K)** Quantification using ImageJ software revealed a significant increase in GFP expression in the CO_2 group as compared with the air inhalation group. $^*p < 0.05$ vs. air controls ($n = 3$ slices per animal from 5 mice/group). Double-labeled GFP-IBA-1 cells (arrows) and single-labeled cells (arrowheads) are indicated. Scale bar = 20 μm.

selective CO_2-evoked regulation of TDAG8 promoter activity within the SFO and potential recruitment of the receptor in CO_2 responses.

Attenuation of CO_2-Evoked Freezing and Contextual CO_2-Conditioned Freezing in TDAG8-Deficient Mice

Freezing [an established measure of fear and panic-like behavior in rodents (8,32)] was used to evaluate behavioral responses to CO_2 in TDAG8$^{+/+}$/TDAG8$^{-/-}$ mice. After a CO_2 dose-response challenge, freezing was reduced in TDAG8$^{-/-}$ mice relative to TDAG8$^{+/+}$ littermates on day 1 (Figure 2B). Two-way ANOVA revealed a significant main effect of genotype ($F_{1,54} = 10.45$; $p < .05$) and treatment ($F_{2,54} = 91.36$; $p < .05$) with no genotype × treatment interaction ($p > .05$), because both genotypes elicited higher freezing to 10% relative to 5% CO_2. Bonferroni post hoc tests revealed significant differences between genotypes ($p < .05$) at both CO_2 concentrations. Neither group froze during air inhalation in the test chamber (Figure 2B). TDAG8 disruption does not impact home cage or novelty-induced motor activity (33), ruling out genotype-associated motor deficits. Fear evoked by psychogenic threats (predator exposure, foot shocks), neuroendocrine stress, or anxiety-like or nociceptive responses were not affected by TDAG8 deficiency (Supplemental Figure S3). Administration of bicarbonate (intraperitoneally) before CO_2 inhalation to minimize acidosis significantly attenuated CO_2-evoked freezing (Supplemental Figure S4; $t_{10} = 4.584$; $p < .05$ vs. saline), suggesting that acidosis (H^+) was required for CO_2-evoked freezing.

Re-exposure to the testing context on day 2 evoked significant freezing in TDAG8$^{+/+}$ mice with prior CO_2 exposure (Figure 2C). This conditioned freezing response was blunted significantly in TDAG8$^{-/-}$ mice. A significant genotype (two-way ANOVA, $F_{1,54} = 9.613$; $p < .05$) and treatment ($F_{2,54} = 23.84$; $p < .05$) effect, but no genotype × treatment interaction ($p > .05$), was observed. Post hoc analysis revealed significant differences between groups ($p < .05$). Negligible freezing was observed if CO_2-exposed mice were placed in a neutral context on day 2 ($p > .05$) (Figure 2D), suggesting that CO_2 evoked conditioned and not generalized fear.

Attenuated CO_2-Evoked Sympathetic Responses but Normal Ventilatory Responses in TDAG8-Deficient Mice

Cardiovascular recordings via radiotelemetry revealed no significant genotype differences in baseline BP, heart rate, or motor activity ($p > .05$ vs. TDAG8$^{+/+}$; Supplemental Figure S5). On exposure to 5% CO_2, TDAG8$^{+/+}$ mice showed an increase in BP over mean pre-CO_2 response that was attenuated significantly in TDAG8$^{-/-}$ mice (Figure 2F). Repeated-measures two-way ANOVA revealed a significant effect of genotype ($F_{1,70} = 20.13$; $p < .05$), but no time or genotype × time interaction ($p > .05$ vs. TDAG8$^{+/+}$). CO_2-evoked bradycardia was not affected by genotype (Figure 2G) ($p > .05$ vs. TDAG8$^{+/+}$). No significant differences in activity during CO_2 inhalation were noted (Figure 2H). Re-exposure to the context (day 2) elicited comparable increases in BP, heart rate, and similar motor activity in TDAG8$^{+/+}$ and TDAG8$^{-/-}$ mice (Figure 2I–K; $p > .05$ vs. TDAG8$^{+/+}$).

Whole-body plethysmography revealed increased ventilatory rate when inspired air was switched from room air to 5% CO_2. Both genotypes exhibited similar hypercapnia-induced increase in ventilatory rate of 100% to 150% ($p > .05$ vs. TDAG8$^{+/+}$; Supplemental Figure S6). Restoring room air (from 5% to 0% CO_2) returned ventilatory rate to the initial values in both genotypes. Thus, hypercapnic ventilatory responses seem to be intact in TDAG8$^{-/-}$ mice.

TDAG8 Gates CO_2-Evoked Activation of Microglia in the SFO

We next investigated TDAG8-mediated microglial activation within the SFO immediately after CO_2-inhalation. SFO ionized calcium-binding adapter molecule$^+$ cells primarily represent microglia because 1) they exhibit distinctive arborized features and morphologic changes to CO_2 inhalation consistent with microglial activation, and 2) predominance of CD4510^w microglia (>95%) versus CD45^{high} macrophages (<5%) was observed by flow cytometry (Supplemental Figure S7). Thus, myeloid cells within the SFO under basal conditions and after mild hypercapnia predominantly represent microglia, not systemic immune cells. As shown in Figure 3, only CO_2-exposed TDAG8$^{+/+}$ mice elicited an increase in soma size and reduced process length and end points, accepted hallmarks of deramified, activated microglia as compared with TDAG8$^{-/-}$ CO_2 and air groups (Figure 3A–K). For soma size (Figure 3I), two-way ANOVA revealed significant effects of genotype ($F_{1,18} = 4.82$; $p < .05$), treatment ($F_{1,18} = 7.464$; $p < .05$), and genotype × treatment interaction ($F_{1,18} = 6.40$; $p < .05$). For reduced process length (Figure 3J), two-way ANOVA revealed significant effect of genotype ($F_{1,18} = 5.98$; $p < .05$) and treatment ($F_{1,18} = 7.68$; $p < .05$). For reduced process end points per cell (Figure 3K), two-way ANOVA revealed a significant effect of genotype ($F_{1,18} = 51.61$; $p < .05$) and a genotype × treatment interaction ($F_{1,18} = 11.81$; $p < .05$), but no significant treatment effect ($p > .05$). Post hoc analysis revealed significant differences between genotypes ($p < .05$). Microglial cell numbers did not differ between groups (Figure 3L; $p > .05$). TDAG8 deficiency did not impact microglial activation to other immunomodulatory agents such as lipopolysaccharide (Supplemental Figure S8), suggesting selectivity of TDAG8 to CO_2-evoked microglial activation. Consistent with selective TDAG8-associated microglial activation within the SFO, we observed no significant differences ($p > .05$) in CO_2-induced microglial changes in other CVOs such as the OVLT or area postrema (Supplemental Figure S9). Thus, TDAG8 gates CO_2-evoked activation of microglia within the SFO.

Microglial Activation and Inflammatory Cytokine IL-1β Are Obligatory to CO_2-Evoked Freezing

Given the association of TDAG8 with CO_2-evoked behavior and microglial activation, we next tested the requirement of microglial activation in CO_2 responses. Central infusion of the microglial blocker minocycline led to a significant attenuation of CO_2-evoked freezing only in TDAG8$^{+/+}$ mice (Figure 4A). Two-way ANOVA revealed a significant effect of treatment ($F_{1,23} = 6.46$; $p < .05$) and genotype ($F_{1,23} = 18.34$; $p < .05$). Post hoc analysis revealed a significant treatment effect in

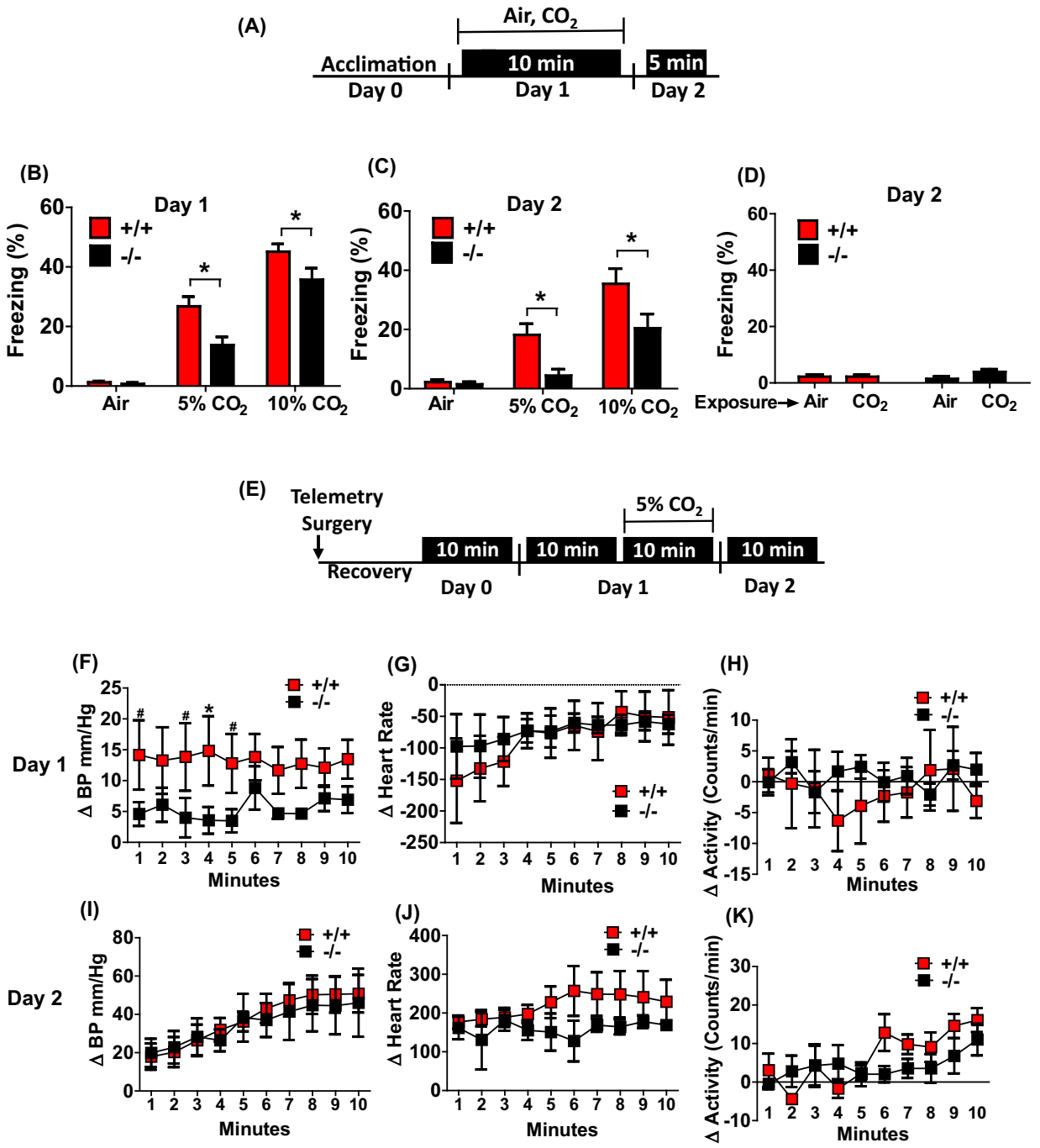

Figure 2. T cell death–associated gene-8 (TDAG8) disruption attenuates fear-associated responses to carbon dioxide (CO_2) inhalation: **(A–D)** CO_2-evoked freezing behavior and **(E–K)** cardiovascular responses are shown. **(A)** Schematic of experimental design for measuring CO_2-evoked freezing and conditioned fear to CO_2 context. **(B)** A significant attenuation of freezing was observed in TDAG8$^{-/-}$ mice after inhalation of 5% and 10% CO_2 on day 1 as compared with TDAG8$^{+/+}$ mice [n/group = 9,11,12($^{+/+}$), 8,10,11($^{-/-}$)]. **(C)** On day 2, significant attenuation of conditioned freezing to CO_2 context was observed in TDAG8$^{-/-}$ mice vs. TDAG8$^{+/+}$ mice [n = 9,11,12($^{+/+}$), 8,10,11($^{-/-}$)]. **(D)** Absence of generalized fear in TDAG8$^{+/+}$ and TDAG8$^{-/-}$ mice exposed to CO_2 inhalation and placed in neutral context 24 hours after exposure. Negligible freezing was observed in CO_2-exposed mice, which was comparable with the air-exposed group. n = 9,10,8,10. **(E)** Schematic of experimental design for measurement of CO_2-evoked cardiovascular activation. Day 1 data represent 5% CO_2-evoked change in cardiovascular parameters (delta Δ) relative to mean response in context 10 minutes before inhalation. **(F)** CO_2-induced elevation in blood pressure (BP) was attenuated significantly in TDAG8$^{-/-}$ vs. TDAG8$^{+/+}$ mice (n = 5). **(G)** No significant difference in heart rate was observed between genotypes. **(H)** TDAG8$^{+/+}$ and TDAG8$^{-/-}$ mice showed no differences in activity during CO_2 inhalation. Day 2 data represent cardiovascular response on exposure to context alone, relative to baseline (defined as mean 2-hour response just before experimenter entry to the animal room). **(I)** For BP, a significant effect of time, but no significant effect of genotype, was observed. **(J)** No significant effect on heart rate was observed. **(K)** Motor activity showed a significant effect of time ($p < .05$), but no effect of genotype was observed. All data are mean ± SEM. *$p < .05$ vs. TDAG8$^{+/+}$.

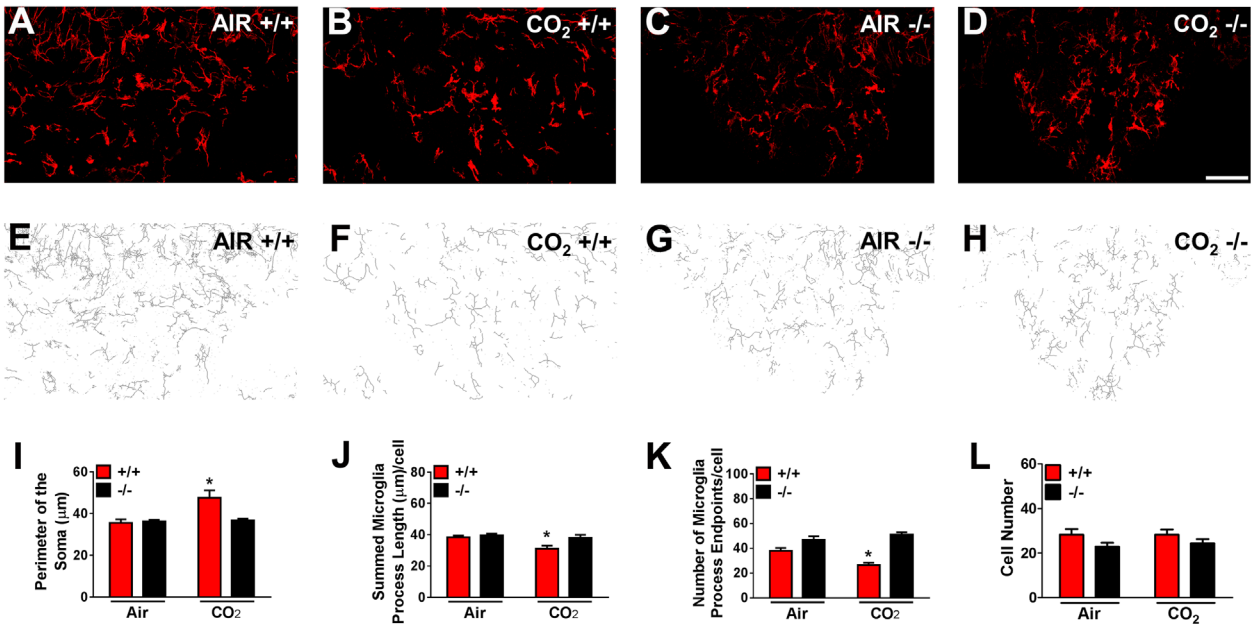

Figure 3. Microglial activation within the subfornical organ after inhalation of 5% carbon dioxide (CO_2) is dependent on T cell death–associated gene-8 (TDAG8) receptor. TDAG8$^{+/+}$ or TDAG8$^{-/-}$ mice were killed after 10 minutes of air or CO_2 inhalation. **(A–D)** Representative fluorescent images of ionized calcium-binding adapter molecule 1 (IBA1)-labeled cells are shown. **(E–H)** Corresponding skeletonized illustrations constructed from maximum intensity projections of images. **(I)** A significant increase in microglial soma perimeter was observed only in CO_2-exposed TDAG8$^{+/+}$ mice vs. TDAG8$^{-/-}$ and air-exposed groups. No significant differences were present in the air-inhalation cohorts. **(J)** Microglia process length showed significant differences between genotypes and treatment effect. **(K)** Process end points per cell revealed a significant difference between genotypes, but treatment did not reach significance. **(L)** No significant differences were observed in the number of microglia between air and CO_2 inhalation groups for both genotypes. All data are mean ± SEM from 3 slices/animal, $n = 6$. *$p < .05$ vs. other groups. Scale bar = 20 μm.

TDAG8$^{+/+}$ mice ($p < .05$). Minocycline had no significant effects in TDAG8$^{-/-}$ mice ($p > .05$), likely because of the absence of CO_2-evoked microglial activation in these mice. Minocycline treatment also reduced CO_2-evoked microglial activation in the SFO (Figure 4B). A significant reduction of microglial soma size ($t_{10} = 2.608$; $p < .05$ vs. aCSF, unpaired t test) and significant increase in process length ($t_{11} = 2.270$; $p < .05$ vs. aCSF) were observed. Collectively, these data support recruitment of TDAG8-dependent microglial activation in the expression of CO_2-evoked freezing.

In response to physiological insults, microglia release proinflammatory cytokines. Significantly reduced IL-1β concentrations were observed in the SFO of TDAG8$^{-/-}$ mice (Figure 4C; $t_6 = 4.280$; $p < .05$ vs. TDAG8$^{+/+}$ mice, unpaired t test). No significant genotype differences in proinflammatory cytokines were observed in other brain regions such as OVLT and amygdala (Supplemental Figure S10A; $p > .05$ vs. TDAG8$^{+/+}$). Central infusion of IL-1β evoked significant freezing in air-exposed TDAG8$^{+/+}$ and TDAG8$^{-/-}$ mice (Figure 4D). Two-way ANOVA revealed a significant effect of treatment ($F_{1,41} = 20.1$; $p < .05$), but no genotype or genotype × treatment interaction ($p > .05$). Intracerebroventricular infusion of the IL-1β antagonist IL-1RA resulted in a significant attenuation of CO_2-evoked freezing (Figure 4E; $t_8 = 2.3$; $p < .05$ vs. aCSF, unpaired t test). Furthermore, IL-1β restored freezing behavior that was attenuated in minocycline-treated mice compared with CO_2-exposed aCSF-treated mice (Figure 4F; $F_{2,29} = 8.424$; $p < .05$, one-way ANOVA). Post hoc analysis revealed that minocycline-IL-1β–treated mice were significantly different from minocycline-only–treated mice ($p < .05$), but not with vehicle group. The increased freezing response was not the result of IL-1β effects on sickness behavior, because motor activity after IL-1β alone remained unchanged for the duration of our behavioral measurement (Supplemental Figure S10B; $p > .05$ vs. aCSF).

Microglial Acid-Sensor TDAG8 Gates CO_2-Chemosensitive Firing Response of SFO Neurons

Translation of microglial acid-sensing via TDAG8 to behavior and sympathetic activation would require neuronal firing. We hypothesized that SFO neurons would exhibit CO_2-chemosensitive responses, dependent on TDAG8 and IL-1β. Firing rate responses of SFO neurons to hypercapnia were studied in TDAG8$^{+/+}$ and TDAG8$^{-/-}$ mice using whole-cell patch clamping (Figure 5A, B). Exposure to 7.5% and 10% CO_2 increased the firing rate of SFO neurons in TDAG8$^{+/+}$ slices, which reversed on return to normocapnia. Similar measurements in TDAG8$^{-/-}$ mice showed no change in firing rate of SFO neurons to CO_2 (Figure 5B). The spontaneous firing rate was increased significantly in TDAG8$^{+/+}$ mice (Figure 5C, red bars). Five of 9 cells (55%) for 7.5% and 6 of 13 cells (46%) for 10% were CO_2 responsive. In contrast, no CO_2-responsive SFO neurons were observed in TDAG8$^{-/-}$ mice at either concentration (7.5% CO_2, 0/8; 10% CO_2, 0/8; Figure 5C, black bars). Unpaired t test revealed significant genotype differences for 7.5% ($t_{11} = 3.314$; $p < .05$ vs. TDAG8$^{+/+}$) and 10% CO_2

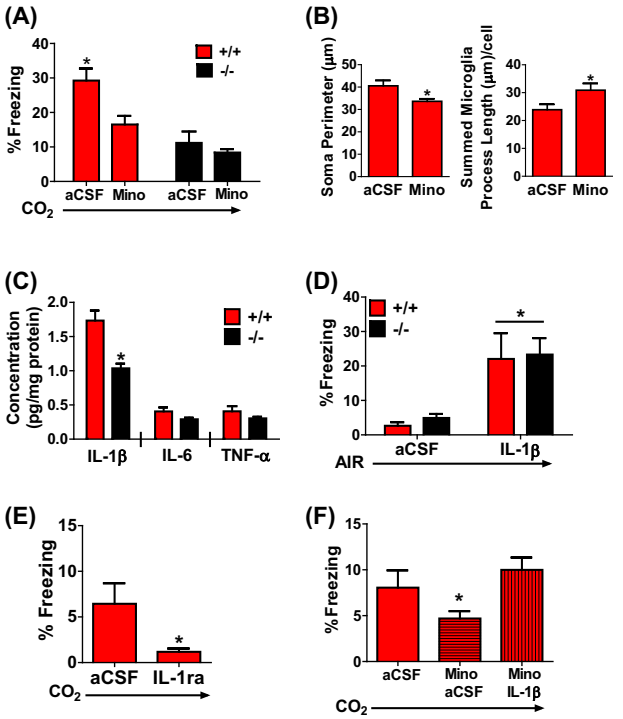

Figure 4. Microglial activation and proinflammatory cytokine interleukin (IL)-1β are associated with carbon dioxide (CO_2) inhalation-evoked fear. **(A)** Administration of minocycline (Mino) attenuates 5% CO_2-evoked freezing in T cell death–associated gene-8 (TDAG8)$^{+/+}$ mice (n = 6–8). No significant effect of Mino was observed in TDAG8$^{-/-}$ mice (n = 6–8). A significant genotype and treatment effect was observed. **(B)** CO_2-evoked microglial activation in the subfornical organ (SFO) of TDAG8$^{+/+}$ mice was reduced significantly in Mino-treated mice. A significant reduction of microglial soma size (left panel) and a significant increase in microglia process length (right panel) was observed (n = 6–7/group; 3 slices/animal). **(C)** A significant reduction in SFO IL-1β concentration was observed in TDAG8$^{-/-}$ mice (n = 4). Other proinflammatory cytokines, IL-6, and tumor necrosis factor alpha (TNFα) in the SFO were not significantly different between genotypes ($p > .05$). **(D)** Sufficiency of IL-1β: central (intracerebroventricular [icv]) infusion of IL-1β evokes significant freezing in air-exposed TDAG8$^{+/+}$ and TDAG8$^{-/-}$ mice. Significant effect of treatment, but no genotype differences, were observed (n = 8–14). **(E)** Necessity of IL-1β: central (icv) infusion of IL-1RA (antagonist of IL-1β) before CO_2 inhalation significantly attenuates freezing (n = 5). **(F)** Central IL-1β infusion restores CO_2-evoked fear in minocycline-treated mice (n = 7–16). Note: Lower magnitude of freezing in all groups shown in **(E)** and **(F)** may be contributed by infusion of agents minutes before behavior. All data are mean ± SEM. *$p < .05$. aCSF, artificial cerebrospinal fluid.

($t_{12} = 4.25$; $p < .05$ vs. TDAG8$^{+/+}$). The lack of firing response to hypercapnia in TDAG8$^{-/-}$ SFO neurons was not the result of compromised neuronal integrity because similar membrane properties were observed between genotypes (Supplemental Figure S11A–C; $p > .05$). CO_2-chemosensitive responses were not TDAG8 dependent in other chemosensory areas such as the locus coeruleus and area postrema (Supplemental Figure 11D–E; $p > .05$). Importantly, IL-1RA significantly attenuated CO_2-evoked firing of SFO neurons (Figure 5D) ($t_8 = 3.602$; $p < .05$ vs. TDAG8$^{+/+}$, unpaired t test), underscoring the necessity of IL-1β for CO_2-evoked neuronal firing in the SFO. Collectively, CO_2-chemosensitve neuronal activation in the SFO is dependent on microglial acid-sensor TDAG8 and IL-1β.

DISCUSSION

Our results delineate a novel mechanism whereby an interoceptive threat (CO_2) elicits fear-relevant behavioral and physiological responses via microglia. CO_2-evoked responses are mediated by a microglial acid-sensing G protein-coupled receptor (TDAG8) in the subfornical organ, a brain region critical for monitoring the internal milieu. Microglial proinflammatory responses may constitute a unique chemosensory system for the detection of homeostatic threats such as CO_2 inhalation of relevance to panic pathophysiological mechanisms.

The acid-sensing TDAG8 receptor is localized to microglia in the sensory CVOs, areas strategically positioned near the brain ventricular system to sense homeostatic fluctuations in the body and brain (34). The SFO can detect circulating cardiovascular and metabolic signals that influence the excitability of single SFO neurons (35). Consistent with this study, previous work links the SFO with panic-like responses to intravenous lactate (20,21). The SFO may be a primary locus for detecting interoceptive challenges relevant to panic.

TDAG8 receptor deficiency led to attenuated CO_2-evoked freezing and sympathetic responses. Rising CO_2 concentrations lead to acidosis, creating a state of homeostatic imbalance resulting in defensive behavioral responses (6,8,32). CO_2-evoked freezing is not completely attenuated in TDAG8$^{-/-}$ mice, suggesting additional acid sensors [such as the acid-sensing ion channel 1 in the amygdala (8) or acid sensing 5-HT neurons in the periaqueductal gray (36)] also may contribute. Acid-sensing ion channel 1 regulates CO_2-evoked freezing at higher (10%) concentrations (8). TDAG8 may be a low-threshold CO_2 sensor relevant to sensitized CO_2 responding observed in PD patients. Higher prevalence of panic attacks at low (5%–7.5%) CO_2 is observed in panic patients, whereas approximately 10% or higher concentrations may affect healthy individuals (3). Having multiple CO_2 sensors enables a broad-spectrum sensing system that may detect a specific range of pH alteration (37).

In addition to evoking spontaneous responses during inhalation, CO_2 also acts as an unconditioned stimulus to produce conditioned freezing specific to exposure context, a response attenuated in TDAG8$^{-/-}$ mice. CO_2-evoked conditioning response also is relevant to PD, because associative learning following panic attacks results in fear and avoidance of panic-associated contexts (38).

Heart rate or ventilatory responses to CO_2 are not affected by TDAG8 deficiency. Modulation of pressor, but not heart rate, responses by TDAG8 may result from a dissociation of sympathetic and parasympathetic drives after CO_2. Increased BP to CO_2 results from an activation of the sympathetic nervous system via central chemoreceptors, whereas changes in heart rate are the result of a secondary reflex activation of the parasympathetic nervous system via arterial baroreceptors (39). TDAG8 does not seem to regulate ventilation [or respiratory control may involve redundant mechanisms (40)]. Studies with acid-sensing ion channel 1$^{-/-}$ mice and delta opioid receptor$^{-/-}$ mice (another model of panic-like responses) also report intact ventilatory responses to CO_2 inhalation (8,41). Compensatory mechanisms during development may have contributed to the unaltered respiratory responsiveness to CO_2.

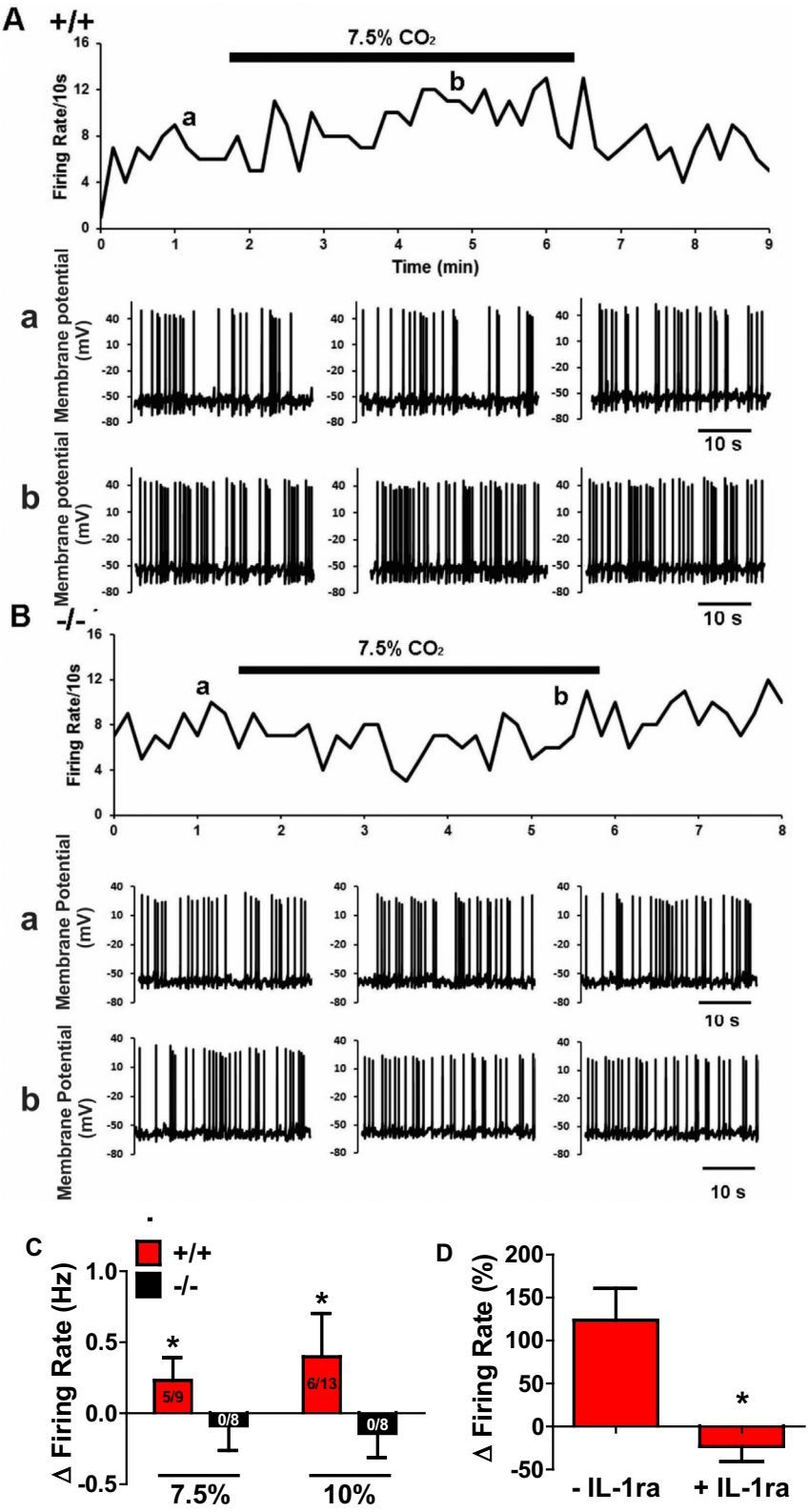

Figure 5. Carbon dioxide (CO_2)-evoked firing of subfornical organ (SFO) neurons is dependent on T cell death–associated gene-8 (TDAG8) and interleukin (IL)-1β. **(A)** Representative trace of an SFO neuron from a TDAG8$^{+/+}$ mouse showing an increase in spontaneous firing rate on exposure to 7.5% CO_2. The upper panel shows the time course of the effect of 7.5% CO_2 on the integrated firing rate. The lower panels show representative traces of spontaneous firing **(a)** before and **(b)** during application of 7.5% CO_2. **(B)** Representative trace of an SFO neuron from a TDAG8$^{-/-}$ mouse. Spontaneous firing rate did not change in the presence of 7.5% CO_2. The lower panels show representative traces of spontaneous firing **(a)** before and **(b)** during application of 7.5% CO_2. **(C)** Histogram summarizing the effects of CO_2 on firing rate of SFO neurons. Each bar represents the mean ± SEM with *n* values (CO_2-responsive neurons/total neurons) shown. Spontaneous firing rate was increased significantly in TDAG8$^{+/+}$ mice on exposure to 7.5% and 10% CO_2 (red bars). Negligible change in firing rate of any TDAG8$^{-/-}$ SFO neurons (black bars) was observed after exposure to 7.5% or 10% CO_2. **(D)** Mean change in firing rate during exposure to 7.5% CO_2 in SFO neurons (left) before and after application of IL-1β receptor antagonist (right) IL-1RA in TDAG8$^{+/+}$ mice that show CO_2-chemosensitive neuronal firing responses in the SFO ($n = 5$). Traces shown in **(A)** and **(B)** are from representative experiments that were repeated at least 5 times. All data are mean ± SEM. *$p < .05$.

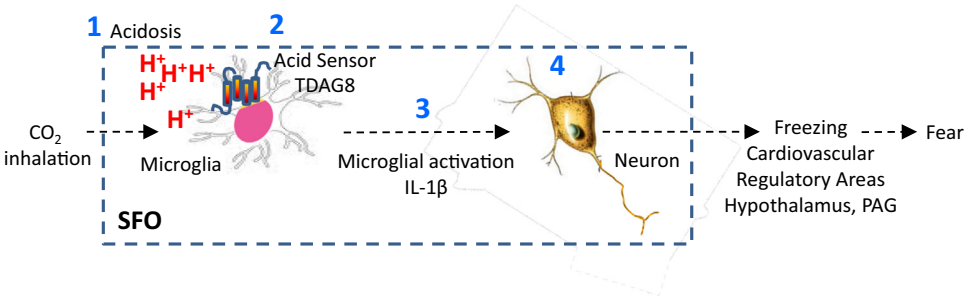

Figure 6. Potential mechanism of carbon dioxide (CO_2)-evoked fear via microglial acid sensor T cell death–associated gene-8 (TDAG8). **(1)** Acidosis (H^+) generated from CO_2 is the likely chemosensory signal because bicarbonate administration attenuates CO_2-evoked responses. **(2)** Microglial acid sensing TDAG8 receptor gates CO_2-evoked activation of microglia and neuronal firing responses within the subfornical organ (SFO) and is recruited in CO_2-evoked behavioral and cardiovascular manifestations of fear. In support, TDAG8-deficient mice have attenuated CO_2-induced freezing and cardiovascular response, reduced microglial activation in the SFO, and negligible neuronal firing responses to CO_2. **(3)** Microglial activation participates in CO_2-evoked fear because pretreatment with minocycline attenuates freezing behavior, as well as microglial activation in the SFO. Proinflammatory cytokine interleukin (IL)-1β is the likely effector because IL-1RA blocks CO_2-evoked fear as well as CO_2-induced firing of SFO neurons. Additionally, central IL-1β infusion is sufficient for evoking freezing response. Consistent with these data, IL-1β rescues CO_2-evoked fear in minocycline-treated mice and TDAG8$^{-/-}$ mice have a selective reduction of IL-1β in the SFO. **(4)** CO_2-evoked chemosensory neuronal firing rate in the SFO is ablated in TDAG8$^{-/-}$ mice, suggesting that TDAG8 acid sensing (and associated microglial inflammatory response) may gate neuronal activation in the SFO. Neurons within the SFO have efferent projections to effector areas such as hypothalamus or periaqueductal gray (43,44) that can regulate freezing and autonomic responses associated with fear. PAG, periaqueductal gray.

Our study outlines a microglial mechanism responsible for CO_2 sensing and its translation to fear-relevant behavior. Recruitment in CO_2 sensing is consistent with microglial tissue surveillance and homeostatic regulation. Our observations of rapid microglial activation in the SFO by CO_2 are consistent with reports of rapid cell swelling and redistribution of actin cytoskeleton of microglia exposed to acidosis in vitro (14,15). Microglial responsivity to an imminent homeostatic survival threat may occur rapidly. SFO microglia in TDAG8$^{-/-}$ mice were not activated by CO_2 inhalation, suggesting that TDAG8 gates microglial activation. Furthermore, minocycline attenuated CO_2-evoked freezing in a TDAG8-dependent manner, highlighting the necessity for TDAG8-associated microglial activation in this effect. Moreover, minocycline treatment attenuated microglial activation within the SFO, further supporting the association of microglial activation with CO_2-evoked responses.

Our studies implicate IL-1β as an effector in microglial TDAG8-mediated freezing to CO_2 inhalation. Physiological responses to the proinflammatory cytokine IL-1β are mediated primarily via the SFO (42). In agreement with selective effects of CO_2 on TDAG8 regulation and microglial activation in the SFO, we observed an SFO-selective reduction of IL-1β in TDAG8$^{-/-}$ mice. Restoration of CO_2-evoked freezing in minocycline-treated mice supplemented with IL-1β further suggests that it acts downstream of microglial activation. Importantly, antagonism of IL-1β attenuated CO_2-evoked freezing, suggesting that necessity and IL-1β infusion was sufficient in evoking freezing in the absence of CO_2. Finally, CO_2-evoked activation of SFO neurons (an effect abolished in TDAG8$^{-/-}$ mice) was dependent on IL-1β. Collectively, our data strongly support SFO IL-1β as the primary effector in CO_2-evoked freezing.

Our study provides the first evidence of CO_2 chemosensing within the SFO, representing a rostral extension of the primitive brain stem CO_2 chemosensory system (3). Neuroanatomic studies have mapped direct efferent connections of the SFO to principal effector sites such as the lateral and dorsomedial hypothalamus (43) and the periaqueductal gray (44), established sites for cardiovascular control and freezing behavior, respectively. Consequently, CO_2-mediated neuronal activation in the SFO then may lead to behavioral and cardiovascular responses to CO_2 inhalation. Selectivity of the SFO in CO_2-evoked effects is intriguing, especially given that TDAG8 expression is observed in other sensory CVOs. The basis of this selectivity is not evident; however, differential expression of carbonic anhydrase isoforms (45) between CVOs may contribute to differences in the efficacy of proton production from CO_2 impacting the dynamics of pH shifts within CVOs. Although our data support the SFO as a primary site for CO_2 responses mediated by microglial TDAG8 receptor, future studies on SFO-targeted interventions are warranted to establish this area further as a key acid-chemosensory site relevant to panic.

Figure 6 illustrates a potential mechanism underlying CO_2-evoked responses via microglial acid sensor TDAG8. Collectively, our findings are relevant to fear and panic pathophysiology. The microglial TDAG8 acid chemosensory system provides a homeostatic threat detection mechanism housed in an area known for monitoring the internal milieu for ionic imbalance. Existence of homeostatic chemosensory systems distinct from psychogenic fear and stress modulatory pathways is supported by expression of intense fear and panic in Urbach-Wiethe patients with damaged amygdala (9). Acid-base disturbances reported in PD patients (46,47) may recruit TDAG8 for translation to fear-associated responses. Although direct analysis for TDAG8 gene polymorphism localized on chromosome 14q31–q32 in PD has not been undertaken, linkage studies in probands with PD and phobias revealed a significant association of chromosome 14 with the disorder (48). Given the relevance of gene × environment interactions in the development of CO_2 hypersensitivity (49), it would be important to assess TDAG8 gene × environment interaction effects on CO_2 sensitivity. Regulation of TDAG8-mediated responses by drugs such as selective serotonin reuptake inhibitors that impact panic symptoms and CO_2 sensitivity will strengthen translational validity of this mechanism. Our data also highlight a potential role for microglial activation and inflammation in panic pathophysiologic mechanisms. Although the contribution of innate immune processes in PD patients or

its comorbidity with inflammatory conditions has not been investigated systematically, a recent National Comorbidity Survey–Replication study reported significantly high comorbidity of PD with conditions associated with inflammation such as rheumatoid arthritis and chronic pain (50). Elevated proinflammatory cytokines were reported in PD (51), although more recently, an association of proinflammatory markers with anxiety disorders in general, but not specific to PD, was reported (52). Alternatively, it is also possible that inflammation in PD is a state-dependent, transient phenomenon that may be difficult to capture in a clinical sample.

In conclusion, our data reveal a unique acid-chemosensory mechanism gated by the acid-sensing TDAG8 receptor on microglia within the subfornical organ, a site accessible to systemic and central milieu. Active engagement of innate immune cells in the detection of homeostatic pH threat may provide novel mechanistic insights into the genesis of fear and panic attacks.

ACKNOWLEDGMENTS AND DISCLOSURES

This work was supported by the National Institute of Mental Health Grant Nos. R01-MH093362 and R21MH083213 (to RS).

We thank Laura Bailey, Kyle Brotkowski, and James B. Chambers for the excellent technical assistance; Dr. Yvonne Ulrich-Lai, University of Cincinnati, for help with the analysis of telemetry data; Dr. Lynn K. Hartzler, Wright State University, for advice and help on plethysmography experiments; Alyssa Sproles, Cincinnati Children's Hospital Medical Center, for assistance with the BioPlex cytokine assays; and Dr. Owen Witte and Dr. Chris Radu, University of California, Los Angeles, for TDAG8-deficient mice ($TDAG8^{-/-}$).

The authors report no biomedical financial interests or potential conflicts of interest

ARTICLE INFORMATION

From the Department of Psychiatry and Behavioral Neuroscience (LLV, SG, JLM, RLA, JR, JPH, RS), Neuroscience Graduate Program (LLV, SG, JPH, RS), University of Cincinnati, Cincinnati; Department of Neuroscience, Cell Biology and Physiology (K-YL, CAR-R, RWP), and Department of Biological Sciences (JMS), Wright State University, Dayton; Division of Immunobiology (IPL), Children's Hospital Medical Center, Cincinnati; and Veterans Affairs (VA) Medical Center (RS), Cincinnati, Ohio; and Department of Animal Morphology and Physiology (LGAP), São Paulo State University, FCAV, Jaboticabal, São Paulo, Brazil.

Address correspondence to Renu Sah, Ph.D., Department of Psychiatry & Behavioral Neuroscience, University of Cincinnati, Metabolic Disease Institute, 2180 East Galbraith Road, Cincinnati, OH 45237; E-mail: sahr@uc.edu.

Received Oct 13, 2015; revised Apr 8, 2016; accepted Apr 13, 2016.

Supplementary material cited in this article is available online at http://dx.doi.org/10.1016/j.biopsych.2016.04.022.

REFERENCES

1. Johansen JP, Cain CK, Ostroff LE, LeDoux JE (2011): Molecular mechanisms of fear learning and memory. Cell 147:509–524.
2. Orsini CA, Maren S (2012): Neural and cellular mechanisms of fear and extinction memory formation. Neurosci Biobehav Rev 36:1773–1802.
3. Colasanti A, Esquivel G, Schruers KJ, Griez EJ (2012): On the psychotropic effects of carbon dioxide. Curr Pharm Des 18:5627–5637.
4. Papp L, Klein DF, Gorman JM (1993): Carbon dioxide hypersensitivity, hyperventilation, and panic disorder. Am J Psychiatry 150:1149–1157.
5. Rassovsky Y, Kushner MG (2003): Carbon dioxide in the study of panic disorder: Issues of definition, methodology, and outcome. J Anxiety Disord 17:1–32.
6. Magnotta VA, Heo H-YY, Dlouhy BJ, Dahdaleh NS, Follmer RL, Thedens DR, *et al*. (2012): Detecting activity-evoked pH changes in human brain. Proc Natl Acad Sci U S A 109:8270–8273.
7. Loeschcke HH (1982): Central chemosensitivity and the reaction theory. J Physiol 332:1–24.
8. Ziemann AE, Allen JE, Dahdaleh NS, Drebot II, Coryell MW, Wunsch AM, *et al*. (2009): The amygdala is a chemosensor that detects carbon dioxide and acidosis to elicit fear behavior. Cell 139:1012–1021.
9. Feinstein JS, Buzza C, Hurlemann R, Follmer RL, Dahdaleh NS, Coryell WH, *et al*. (2013): Fear and panic in humans with bilateral amygdala damage. Nat Neurosci 16:270–272.
10. Hanisch U-KK, Kettenmann H (2007): Microglia: active sensor and versatile effector cells in the normal and pathologic brain. Nat Neurosci 10:1387–1394.
11. Walker FR, Beynon SB, Jones KA, Zhao Z, Kongsui R, Cairns M, Nilsson M (2014): Dynamic structural remodelling of microglia in health and disease: A review of the models, the signals and the mechanisms. Brain Behav Immun 37:1–14.
12. Kreutzberg GW (1996): Microglia: a sensor for pathological events in the CNS. Trends Neurosci 19:312–318.
13. Kettenmann H, Hanisch U-K, Noda M, Verkhratsky A (2011): Physiology of microglia. Physiol Rev 91:461–553.
14. Morihata H, Nakamura F, Tsutada T, Kuno M (2000): Potentiation of a voltage-gated proton current in acidosis-induced swelling of rat microglia. J Neurosci 20:7220–7227.
15. Faff L, Nolte C (2000): Extracellular acidification decreases the basal motility of cultured mouse microglia via the rearrangement of the actin cytoskeleton. Brain Res 853:22–31.
16. McGuire J, Herman JP, Ghosal S, Eaton K, Sallee FR, Sah R, *et al*. (2009): Acid-sensing by the T cell death-associated gene 8 (TDAG8) receptor cloned from rat brain. Biochem Biophys Res Commun 386:420–425.
17. Radu CG, Nijagal A, McLaughlin J, Wang L, Witte ON (2005): Differential proton sensitivity of related G protein-coupled receptors T cell death-associated gene 8 and G2A expressed in immune cells. Proc Natl Acad Sci U S A 102:1632–1637.
18. Johnson AK, Gross PM (1993): Sensory circumventricular organs and brain homeostatic pathways. FASEB J 7:678–686.
19. Johnson PL, Sajdyk TJ, Fitz SD, Hale MW, Lowry CA, Hay-Schmidt A, Shekhar A (2013): Angiotensin II's role in sodium lactate-induced panic-like responses in rats with repeated urocortin 1 injections into the basolateral amygdala: amygdala angiotensin receptors and panic. Prog Neuropsychopharmacol Biol Psychiatry 44:248–256.
20. Shekhar A, Keim SR (1997): The circumventricular organs form a potential neural pathway for lactate sensitivity: implications for panic disorder. J Neurosci 17:9726–9735.
21. Shekhar A, Sajdyk TS, Keim SR, Yoder KK, Sanders SK (1999): Role of the basolateral amygdala in panic disorder. Ann N Y Acad Sci 877:747–750.
22. Radu CG, Cheng D, Nijagal A, Riedinger M, McLaughlin J, Yang LV, *et al*. (2006): Normal immune development and glucocorticoid-induced thymocyte apoptosis in mice deficient for the T-cell death-associated gene 8 receptor. Mol Cell Biol 26:668–677.
23. Leibold NK, Viechtbauer W, Goossens L, De Cort K, Griez EJ, Myin-Germeys I, *et al*. (2013): Carbon dioxide inhalation as a human experimental model of panic: The relationship between emotions and cardiovascular physiology. Biol Psychol 94:331–340.
24. Ulrich-Lai YM, Christiansen AM, Ostrander MM, Jones AA, Jones KR, Choi DC, *et al*. (2010): Pleasurable behaviors reduce stress via brain reward pathways. Proc Natl Acad Sci U S A 107:20529–20534.
25. Patrone LGA, Bicego KC, Hartzler LK, Putnam RW, Gargaglioni LH (2014): Cardiorespiratory effects of gap junction blockade in the locus coeruleus in unanesthetized adult rats. Respir Physiol Neurobiol 190:86–95.
26. Neigh GN, Karelina K, Glasper ER, Bowers SLK, Zhang N, Popovich PG, DeVries AC (2009): Anxiety after cardiac arrest/cardiopulmonary resuscitation: exacerbated by stress and prevented by minocycline. Stroke 40:3601–3607.

27. Goshen I, Kreisel T, Ounallah-Saad H, Renbaum P, Zalzstein Y, Ben-Hur T, *et al*. (2007): A dual role for interleukin-1 in hippocampal-dependent memory processes. Psychoneuroendocrinology 32:1106–1115.
28. Norman GJ, Zhang N, Morris JS, Karelina K, Berntson GG, DeVries a C (2010): Social interaction modulates autonomic, inflammatory, and depressive-like responses to cardiac arrest and cardiopulmonary resuscitation. Proc Natl Acad Sci U S A 107:16342–16347.
29. Morrison HW, Filosa JA (2013): A quantitative spatiotemporal analysis of microglia morphology during ischemic stroke and reperfusion. J Neuroinflammation 10:4.
30. Cutando L, Busquets-Garcia A, Puighermanal E, Gomis-González M, Delgado-García JM, Gruart A, *et al*. (2013): Microglial activation underlies cerebellar deficits produced by repeated cannabis exposure. J Clin Invest 123:2816–2831.
31. Li K-Y, Putnam RW (2013): Transient outwardly rectifying A currents are involved in the firing rate response to altered CO2 in chemosensitive locus coeruleus neurons from neonatal rats. Am J Physiol Regul Integr Comp Physiol 305:R780–R792.
32. Mongeluzi DL, Rosellini RA, Ley R, Caldarone BJ, Stock HS (2003): The conditioning of dyspneic suffocation fear. Effects of carbon dioxide concentration on behavioral freezing and analgesia. Behav Modif 27:620–636.
33. Vollmer LL, Schmeltzer SN, Ahlbrand R, Sah R (2015): A potential role for the acid-sensing T cell death associated gene-8 (TDAG8) receptor in depression-like behavior. Physiol Behav 150:78–82.
34. McKinley MJ, McAllen RM, Davern P, Giles ME, Penschow J, Sunn N, *et al*. (2003): The sensory circumventricular organs of the mammalian brain. Adv Anat Embryol Cell Biol 172:III–XII,1-122, back cover.
35. Mimee A, Smith PM, Ferguson AV (2013): Circumventricular organs: targets for integration of circulating fluid and energy balance signals? Physiol Behav 121:96–102.
36. Severson CA, Wang W, Pieribone VA, Dohle CI, Richerson GB (2003): Midbrain serotonergic neurons are central pH chemoreceptors. Nat Neurosci 6:1139–1140.
37. Jiang C, Rojas A, Wang R, Wang X (2005): CO_2 central chemosensitivity: Why are there so many sensing molecules? Respir Physiol Neurobiol 145:115–126.
38. Lissek S, Rabin S, Heller RE, Lukenbaugh D, Geraci M, Pine DS, Grillon C (2010): Overgeneralization of conditioned fear as a pathogenic marker of panic disorder. Am J Psychiatry 167:47–55.
39. Oikawa S, Hirakawa H, Kusakabe T, Nakashima Y, Hayashida Y (2005): Autonomic cardiovascular responses to hypercapnia in conscious rats: The roles of the chemo- and baroreceptors. Auton Neurosci Basic Clin 117:105–114.
40. Nattie E (2000): Multiple sites for central chemoreception: their roles in response sensitivity and in sleep and wakefulness. Respir Physiol 122: 223–235.
41. Borkowski AH, Barnes DC, Blanchette DR, Castellanos FX, Klein DF, Wilson DA (2011): Interaction between δ opioid receptors and benzodiazepines in CO_2-induced respiratory responses in mice. Brain Res 1396:54–59.
42. Wei S-G, Zhang Z-H, Beltz TG, Yu Y, Johnson AK, Felder RB (2013): Subfornical organ mediates sympathetic and hemodynamic responses to blood-borne proinflammatory cytokines. Hypertension 62:118–125.
43. Swanson LW, Lind RW (1986): Neural projections subserving the initiation of a specific motivated behavior in the rat: new projections from the subfornical organ. Brain Res 379:399–403.
44. Uschakov A, McGinty D, Szymusiak R, McKinley MJ (2009): Functional correlates of activity in neurons projecting from the lamina terminalis to the ventrolateral periaqueductal gray. Eur J Neurosci 30: 2347–2355.
45. Ruusuvuori E, Kaila K (2014): Carbonic anhydrases and brain pH in the control of neuronal excitability. Subcell Biochem 75:271–290.
46. Friedman SD, Mathis CM, Hayes C, Renshaw P, Dager SR (2006): Brain pH response to hyperventilation in panic disorder: Preliminary evidence for altered acid-base regulation. Am J Psychiatry 163: 710–715.
47. Vollmer LL, Strawn JR, Sah R (2015): Acid-base dysregulation and chemosensory mechanisms in panic disorder: A translational update. Transl Psychiatry 5:e572.
48. Gelernter J, Page GP, Bonvicini K, Woods SW, Pauls DL, Kruger S (2003): A chromosome 14 risk locus for simple phobia: Results from a genomewide linkage scan. Mol Psychiatry 8:71–82.
49. Battaglia M, Ogliari A, D'Amato F, Kinkead R (2014): Early-life risk factors for panic and separation anxiety disorder: Insights and outstanding questions arising from human and animal studies of CO_2 sensitivity. Neurosci Biobehav Rev 46(pt 3):455–464.
50. Gadermann AM, Alonso J, Vilagut G, Zaslavsky AM, Kessler RC (2012): Comorbidity and disease burden in the National Comorbidity Survey Replication (NCS-R). Depress Anxiety 29:797–806.
51. Hoge EA, Brandstetter K, Moshier S, Pollack MH, Wong KK, Simon NM (2009): Broad spectrum of cytokine abnormalities in panic disorder and posttraumatic stress disorder. Depress Anxiety 26: 447–455.
52. Vogelzangs N, Beekman ATF, de Jonge P, Penninx BWJH (2013): Anxiety disorders and inflammation in a large adult cohort. Transl Psychiatry 3:e249.